INJURY BIOMECHANICS RESEARCH
Proceedings of the Forty First International Workshop

Development of a 5th Percentile Female Finite Element Model Using a Multi-Modality Image Set

Matthew L. Davis[1,2], Daniel P. Moreno[1,2], Joel D. Stitzel[1,2], F. Scott Gayzik[1,2]

[1]Virginia Tech-Wake Forest University Center for Injury Biomechanics
[2]Wake Forest University School of Medicine, Department of Biomedical Engineering

ABSTRACT

To mitigate the societal impact of vehicle crash, researchers are using a variety of tools, including finite element models. As part of the Global Human Body Models Consortium project, comprehensive medical image and anthropometrical data of the 5th percentile female (F05) were acquired. Height, weight and 15 external anthropomorphic measurements were used to determine subject eligibility. A multi-modality image dataset consisting of CT, MRI and upright MRI medical images was developed to characterize the subject in the supine, seated and standing postures. Surface topography and 52 bony landmarks were also acquired for model assembly. The selected subject closely represented the F05 in terms of height and weight, deviating less than 2% in those measures. For all 15 anthropomorphic measurements, the average subject deviation across all measures was 4.1%. The multi-modality image set was used to develop and assemble skeletal and organ components of the model. Abdominal organ volumes and cortical bone thickness were compared to literature sources where data was available. The dataset used for the development of this model was acquired with the explicit purpose of developing a full-body finite element model of the F05 for the enhancement of injury prediction.

INTRODUCTION

Computational human body modeling for blunt injury prediction and prevention is a growing field within biomechanics. The last 20 years has seen a large increase in the number of human body models being developed at both the full body level (Hayes et al. 2014; Toyota 2010; Yang et al. 2006) and body regional level (DeWit and Cronin 2012; Li et al. 2010; Shin et al. 2012; Soni and Beillas 2013). This growth has been driven by the need to address major public health problems, including vehicular crash. Motor vehicle injuries and fatalities remain a leading public health concern worldwide. In 2013, the World Health Organization reported more than 1.2 million deaths as a result of motor vehicle crashes (W.H.O 2013). Computational tools, such as the finite element method, offer a cost-effective way to evaluate and design

safety systems within a dynamic impact environment. They also have the ability to provide a greater understanding of injury mechanisms and can be used as a basis to calculate injury criteria. Such models, whether they are used for kinematic studies or to model local level trauma, require accurate representation of the body habitus central to the research. To accomplish this, model developers have relied on a number of data sources to accurately represent the human anatomy. For example, external anthropometry and medical imaging databases have been used in the past to assemble subject specific geometries into a model coordinate system (Gayzik et al. 2011; Gayzik et al. 2012).

Traditionally, human body models are developed to represent an average male (50^{th} percentile in terms of height and weight). While these models can provide a valuable assessment of the mid-sized adult male, real world motor vehicle crashes involve occupants of various size, age and gender. In the late 1990's, there was a series of fatalities resulting from airbag related injuries in otherwise low to moderate severity frontal crashes. Upon investigation, it was found that 78% of the fatalities were female, and 82% of the females were less than 163 cm tall (below average height) (Summers et al. 2001). This indicated that vehicle safety features needed to be evaluated for drivers beyond the average sized male, and provided motivation to expand the methods of vehicle safety evaluation. From a regulatory perspective, this was addressed by including the response of a small female anthropomorphic test device (Hybrid III 5^{th} percentile female) to evaluate the ability of vehicle safety devices to protect a wider range of occupants. In an effort to further the ability of computational models to provide comparable data, this study focuses on the development of a model of a female driver in the 5^{th} percentile of height and weight.

Previous research has shown that females are considered to be at a larger risk of sustaining injury during automotive accidents when compared to males (Evans 2001; Morris et al. 1998). Based on a comparison of drivers in the United States and the United Kingdom using the National Automotive Sample System (NASS) and the Cooperative Crash Injury Study (CCIS), Mackay et al. found that the median tolerable delta-V was considerably lower for females than for males at any given severity level on the Abbreviated Injury Scale (AIS) (Mackay and Hassan 1999). A statistical analysis using data from the Master Accident Record System (MARS) has also found that females have a higher percentage of sustaining fatal or disabling injuries as a result of vehicle crash (Ulfarsson and Mannering 2004). To reduce confounding effects of crash severity, Evans et al. reported that females are also at a greater risk of injury compared to males in similar physical impacts (Evans 2001). More specifically, small females are also more likely to sustain chest injuries with a maximum AIS of 2 or greater (Welsh and Lenard). One of the main reasons for this increased risk is the preferred seated posture of small females closer to the wheel as a result of their stature (King and Yang 1995; Manary et al. 1998; Melvin et al. 1993). Increased injuries may also be attributable to lower structural strength within females due to lower bone mineral content (Duma et al. 1999).

Until recently, finite element models of the 5^{th} percentile female (F05) have typically been developed by applying scaling techniques to existing 50^{th} percentile male models, since scan data of such a specific target anthropometry are limited. To scale these models, anthropomorphic relationships are established using external anthropometry databases. For example, the HUMOS2 F05 was produced using European databases of anthropometry to define the external geometry of the body that corresponds to specific percentiles (Serre 2006; Vezin and Verriest 2005). Relationships between internal and external dimensions were then used to develop a statistical method for scaling. Another early model of the small female was developed by Happee et al (Happee et al.). This model was developed using anthropometry from the RAMSIS anthropometry database. In 2003, Iwamoto et al. described the development of the Toyota Total Human Model for Safety (THUMS) small female model (Iwamoto et al. 2003). This model was developed by scaling the THUMS average sized male using anthropometric data of the small female occupant from the University of Michigan (Schneider et al. 1983). However, in order to account for gender differences, thoracic and pelvic regions of the model were developed *ad hoc* to represent the small female. Similarly, Kimpara et al. reported on the development of an early version of the American F05 using data on female geometry from the View Point Datalabs database (Kimpara et al. 2002). However, this model did not include internal organs or female-specific biomechanical properties and was not fully validated. Kimpara et al. later published work on integrating the THUMS F05 with internal organ models from the Wayne State University Human Thorax Model (WSUHTM) for improved thoracic response (Kimpara 2005). More recently, the THUMS AF05 has been improved to include more accurate models of specific internal organs. The geometry for these structures was obtained from high resolution supine computed tomography (CT) scans of a subject representative of the 5^{th} percentile female.

The objectives of this study are two-fold. The first is to present comprehensive image and anthropometrical data of the F05 subject selected in this study. This includes medical images from both CT

and magnetic resonance imaging (MRI) scans to obtain subject specific images in the supine, seated and standing postures. Recent studies have found significant differences in abdominal organ positioning and shape between supine and seated postures (Beillas 2009; Hayes et al. 2013). Therefore, in order to most accurately characterize the shape of internal organs and their position in the spinal frame, medical images need to be obtained in a variety of postures. The second objective is to present the techniques for 3D geometry development and model assembly. This model will be the foundation for the development of the Global Human Body Models Consortium's (GHBMC) F05 finite element model. The consortium's mission is to create and maintain the world's most biofidelic computational human body models. The data presented on the development of the F05 is intended to provide an anatomic reference to engineers and researchers to aid in the advancement of automotive safety.

METHODS

The medical imaging protocol was approved by the Wake Forest University School of Medicine's Institutional Review Board (IRB, #5705). As an initial solicitation for a single individual to represent the 5th percentile female, target height and weight of 150.9 cm and 49 kg were used. The initial screening process was conducted via advertisements with limited anthropometric data self-reported during the phone screen. Once candidates were identified, 15 anthropomorphic measurements were acquired and compared to existing anthropometry values presented by Gordon et al (Gordon et al. 1989). For inclusion in the study, the subject was to be within 5% deviation across all measurements. Applicants also had to be in generally good health and have all organs present. Additional exclusion criteria related to the imaging component of the study, such as claustrophobia and any implanted metals, were also included to ensure subject safety.

Medical Imaging Protocol

The selected subject was carefully screened to ensure safety prior to scanning, and all images were reviewed by a faculty radiologist. In order to fully characterize the subject for model development, a multi-modality image dataset was collected (Gayzik et al. 2009; Gayzik et al. 2011). This dataset was comprised of CT, MRI and upright MRI (uMRI) to obtain images in the supine, seated and standing postures. CT scans allowed for accurate reconstruction of skeletal structures. Seated and standing uMRI scans were used to assemble geometries segmented from the higher resolution supine MRI scans. This approach increased the biofidelity of both the shape and placement of structures for improved response in the subsequent models. Typical scan acquisition parameters have been reported by Davis et al. (Davis et al. 2014). Examples of the multi-modality image dataset can be seen in Figure 1.

CT scans were acquired using a GE LightSpeed, 16-slice scanner. Due to the fast acquisition time, high resolution, and strong contrast for bone, CT scanning were selected as part of the development process. All images were acquired with the scanner in helical mode, with the subject placed in both supine and quasi-seated postures. The inability to achieve a true seated posture was due to limitations presented by the scanner's restrictive bore size (72 cm). Therefore, to place the subject in the quasi-seated position, custom foam and acrylic inserts were attached to the scanning table and were rotated about the Y-axis (per SAE J211) such that the subject fit through the bore. For all scans, the matrix size was 512 mm x 512 mm. The CT scan protocol was established after consulting with a board certified radiologist and was designed to minimize radiation dose. No contrast was used on the subject in this study. Females who were pregnant or did not report the use of a contraceptive were excluded from the study.

Supine MRI images were acquired using a 1.5 Tesla Twin Speed scanner (GE, Milwaukee, WI). A 3D fast spoiled gradient recalled pulse sequence (FSPGR) was used and the ratio of echo time (TE) to repetition time (TR) was selected to have fat and water signals out of phase. This produced images with an enhanced outline between the viscera, fat and muscle for improved segmentation. In order to reduce motion artifact during thoracic and abdominal scan acquisition, the volunteer was trained with breath-holding techniques. Scans for other regions were non-breath held. Scan acquisition parameters were TR = 5.26 ms, TE = 1.8 ms, flip angle = 10^0, and bandwidth = 62.5 MHz. An 8-channel-phased-array body coil was used to collect the majority of the data. For the head and neck however, an 8-channel neurovascular coil was used. Images were primarily collected in the transverse plane, with coronal images obtained for select anatomy in the head and abdomen. Upon completion of image acquisition, all images were reformatted to a matrix size of 512 x 512.

The uMRI scans were obtained using a 0.6 Tesla Fonar Upright MRI (Fonar, Inc., Melville, NY) and Sympusle v.7.0 software. Again, 3D gradient pulse sequences were used to place fat and water out of phase. A quadrature head coil and a set of spine and body coils were used for image acquisition. Acquisition parameters for the uMRI were TR = 14.7 ms, TE = 5.6 ms, flip angle = 30^0, and an acquisition matrix of 200 x 200. Slice thicknesses for acquisition varied from 1.5 mm to 2 mm. Images were acquired in both seated and standing positions. In the seated scans, the seat back angle was set to 23^0. The images taken in the standing posture were of the shoulder, thorax, abdomen and standing knee.

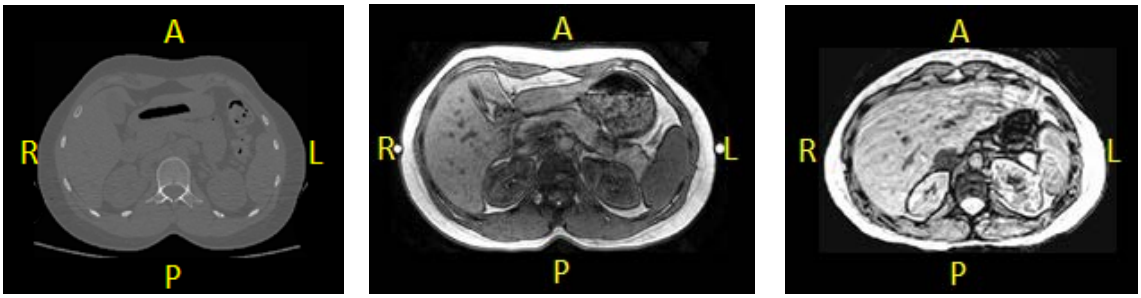

Figure 1. Examples of the Multi-Modality Image Set, a) Axial slice of supine CT, b) Axial slice of supine MRI, c) Axial slice of seated uMRI. Each image was taken at the level of the 3rd lumbar vertebra.

External Anthropometry

A 7-axis 3D FaroArm digitizer (Faro, Platinum Model arm, 2.4 m, Lake Mary, FL) was used for the collection of the subject's surface topography and external landmarks (Gayzik et al. 2012). The landmarks were used to characterize the posture of the subject throughout the body; head (n=9), spine (n=6), thorax (n=9), pelvis (n=5), upper extremity (n=12) and lower extremity (n=14). To facilitate future modeling efforts, this information was collected from the subject in both seated and standing postures. Data were collected in a single session and in the following order: seated landmark data, seated surface data, standing landmark data and standing surface data.

For proper placement in the driving position, a custom, adjustable seat buck and platform were developed (Gayzik et al. 2012). The seat back and pan angles were set to 23^0 from vertical and 14.5^0 from horizontal respectively. Each variable parameter in the buck was set to properly fit the stature of the subject. For future modeling purposes, a local coordinate system was defined using markers on the seat buck with the origin defined as the seat's H-point. This coordinate system was used to define the final model space. To ensure access to the full topography of the subject while in the seated position, the seat back of the buck was divided into halves, allowing for mid-sagittal spinal landmarks to be collected.

After positioning the subject in the buck, a visual target was oriented at the subject's eye level to place the head in the Frankfurt plane. In total, 54 bony landmarks were identified through palpation. Directly following landmark data collection, while the subject was still seated in the buck, a scan of the subject's surface topography was acquired using the FaroArm with an integrated laser attachment. The scan was taken of the right side of the volunteer's body, with major structures on the left side, such as the thigh and shoulder, scanned to validate mirroring. In order to reduce artifact in the scan, the subject wore white, non-reflective, form-fitting clothing. In order to obtain un-deformed body contours, the seat back panels and pans could be removed from their docked positions individually. Because of the time required for data collection and the fact that the patient had to remain still throughout, the data collection was divided into sessions of 20 minutes. Standing data were acquire using similar techniques further described by Gayzik et al (Gayzik et al. 2012).

The external landmarks were symmetrized by fitting a sagittal symmetry plane to the landmark data. Right and left side data points were mirrored across the plane. The transformations of the points were then averaged to establish the final point locations of the extremities. Points found along the mid-sagittal plane of the axial skeleton were projected along the Y axis to the global XZ plane. These points were then defined per the SAE J211 sign convention that was aligned to the mid-sagittal plane, with the origin at the H-point.

Segmentation

After collection of the medical imaging dataset, the images were used to develop 3D representations of the pertinent F05 anatomy for finite element analysis (FEA) model development. Segmentation was used to obtain as much structural information as possible from the medical images. Adjacent image stacks from the same modality were merged into a continuous set of images to properly segment geometries that may have not have been fully represented in one image stack. Mimics software (v16.0, Materialise, Belgium) was used for all segmentations. Segmentation techniques consisted of a mixture of manual and semi-automatic techniques, with the tissue type dictating the approach. Standard segmentation techniques such as region growing, morphological operations, multi-slice interpolation and Boolean operations were also employed as needed (Gayzik et al. 2011).

Bone

The bones of the body were individually segmented. However, fused bones, such as the ilium, ischium and pubic bone, were not separated. To segment bony structures, a semi-automatic method using thresholding techniques was employed. Bone segmentation began by selecting pixels exceeding 226 Hounsfield Units. In regions with small articular spaces, such as with the interface between the thoracic spine and the ribs, the structures were manually separated. Initial segmentations of bony structures were performed using supine CT data. This dataset was preferred for the initial development of 3D bone data due to its high resolution and contrast. To promote accurate assembly, the 3D polygon data obtained from the supine CT was then imported into the image space of the quasi-seated CT and aligned with the corresponding structures using affine transformations. This allowed the higher resolution scans to be used for segmentation and the seated scans to be used for more accurate placement. One limitation to the quasi-seated CT scan was its inability to accurately capture the correct curvature of the lumbar spine in the seated position. In order to overcome this limitation, the assembly data for the lumbar spine was taken from the seated uMRI scans, where a more realistic seated posture was possible due to the open bore nature of the scanner. This coupling of the lumbar spine curvature with the thoracic and cervical spines from the seated CT enabled the full spine to be assembled in the seated position.

Organs

The majority of organ segmentations were manually completed using standard segmenting techniques, including flood fills, region growing and multi-slice interpolation. Supine CT data were used for segmentation of the thoracic organs because the high contrast between the air filled lungs and the surrounding tissues was easily identified via thresholding within the CT scan. In order to outline the heart, a contrast enhanced scan was selected from the Wake Forest University image database and anonymized. The individual was female, with a height of 149 cm, and weight of 49 kg. All remaining organs were segmented using supine MRI data.

Apart from the white matter, all brain structures that will be used in the model were manually segmented. The white matter was automatically segmented using statistical parametric mapping software (SPM5, Functional Imaging Laboratory, University College London). After the voxels had been selected, they were then transformed back into the subject image space and verified against the subject image set.

In order to account for postural effects on the abdominal organs, after segmentation using the supine MRI data, the 3D surfaces of the abdominal organs were transformed into the uMRI image space using affine transformations. The surfaces from the supine data were then used as a basis to adjust for the organ shape variation found in the seated posture. This approach was taken to apply the strengths of both scans to the data set. The supine MRI data were preferable for initial segmentation due to field strength and higher resolution and the seated uMRI was used for its accurate placement and shape. The seated uMRI scans were also used to capture the correct orientation of major abdominal vasculature (such as the inferior vena cava and aorta), the colon and the small bowel.

Assembly

Following completion of bony segmentation and alignment in the seated scans, the skeletal structures were assembled in the model coordinate system. This was completed using affine transformations from the medical image space to align the structures to the bony landmark data in the model space (SAE J211). In order to ensure that characteristics such as spinal curvature were maintained during assembly, the skeleton was moved in segments consisting of the cervical spine, thoracic spine and ribs, and the lumbar spine. The sacrum was also assembled as a segment with the pelvis. An example of the placement and assembly of the cervical spine can be seen in Figure 2.

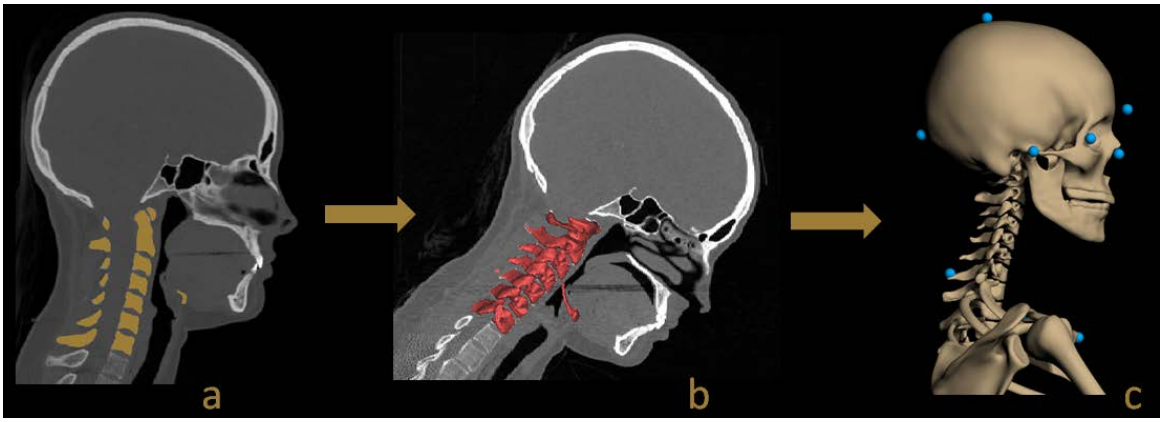

Figure 2. Schematic of model assembly process, a) Cervical spine masks from supine CT segmentation, b) 3D polygon surface data from segmentation placed in the quasi-seated CT image space, c) Cervical spine is transformed as a group into the model space and aligned with the skull and thoracic spine using bony landmarks (blue).

The supine MRI scan was used for assembly of brain structures. To assemble the brain, the skull was first segmented from the supine CT scans and aligned within the supine MRI. Due to contrast deficiencies, the skull could not be directly segmented from the MRI data. The skull was then used to develop a transform from the MRI space to the model space. This transform was used to bring brain structures into the model coordinate system.

To complete the assembly of abdominal organs, the axial skeleton segmented from the supine CT scans was aligned within the seated uMRI scan (Figure 3). Model assembly utilized the placement of the skeletal structures within the seated uMRI to develop transforms for soft tissue in the uMRI image space to the model space. Because the shape and volume of bony structures does not change relative to posture, specific bones or bony segments were used to develop transforms by aligning the bones from the image space to the assembled skeleton in the model coordinate system. For example, a skeletal segment containing portions of the thoracic spine and lumbar spine (T8-L3) and ribs 8-12 was transformed from the uMRI image space to the assembled model skeleton using a best fit alignment algorithm. The resulting transform was then applied to the solid organs of the upper abdomen (liver, kidneys, gallbladder, spleen, stomach and pancreas). Best fit alignments using the pelvis and lumbar spine were used for placement of the colon, small bowel and bladder.

Figure 3. Skeletal structures segmented from supine MRI data (outlined in red) placed in the uMRI image space.

RESULTS

In total, 2 subjects passed the initial screening of height and weight. However, only one of these volunteers passed the secondary screening of external anthropometry measurements from Gordon et al. Ultimately, the selected volunteer (24 years old, female) was a good fit in terms of height and weight (149.9 cm, 48.1 kg) with deviations from the target values of 0.7% and 1.9% respectively. For all 15 measurements, the average subject percent deviation was 4.1% (cutoff for inclusion was 5%). A summary of each

measurement can be seen in Table 1.

Table 1. Anthropometric measurements of the 5th percentile female volunteer

Measurement	Subject	Target (Gordon et al. 1989)	Deviation (%)
Sitting Height	80.0	79.5	0.6
Hip Breadth Sitting	35.6	34.2	3.9
Buttock Knee Length Sitting	52.8	54.2	-2.5
Knee Height Sitting	46.0	47.4	-3.0
Bideltoid Breadth, Sitting	40.6	39.7	2.4
Shoulder-Elbow Length, Standing	33.0	30.8	7.3
Forearm-Hand Length, Standing	40.4	40.6	-0.6
Waist Circumference, Standing	78.2	67.6	15.8
Hip Breadth, Standing	31.2	30.8	1.5
Foot Length, Standing	22.6	22.4	0.8
Head Breadth	14.5	13.7	5.9
Head Length	18.8	17.6	6.6
Head Circumference	53.6	52.2	2.6
Chest Circumference	83.8	81.4	3.0
Neck Circumference	30.5	29.2	4.3

In total, 66 scan series were collected across all modalities for a total of 14,170 images. Using this data, 3D geometries were developed for all skeletal structures and each organ that will be explicitly modeled. The skeleton consists of 182 individual bones. Explicit representations of 32 organs have also been developed, represented by brain, thoracic, and abdominal organs relevant to biomechanical modeling. The following 16 structures are represented within the model of the brain: left and right cerebral hemispheres, corpus callosum, ventricles (3^{rd}, 4^{th}, and lateral), brainstem, fornix, thalamus, cerebellum, falx, tentorium, left and right basal ganglia and the venous sinuses (transverse and superior). Within the thorax and abdomen, 3D representations of the heart (obtained from a contrast-enhanced clinical CT scan), right and left lungs, liver, spleen, right and left kidneys, gallbladder, stomach, colon, duodenum, pancreas and the bladder have been developed. Due to its complicated geometry, the small bowel was developed as a control volume. Volumetric data for a selection of modeled organs have been previously published by Davis et al (Davis et al. 2014). Major vasculature is also represented in these regions, including the aorta, vena cava and hepatic portal vein. The aorta and vena cava were each measured at three discrete points to obtain diametric measurements. The aorta was measured at its superior exit from the heart (26.7 mm), at the inferior portion of the aortic arch (20.1 mm), and parallel to the superior surface of L3 (13.3 mm). The measurements for the vena cava were taken at the superior exit from the heart (17.8 mm), the inferior exit from the liver (20.8 mm), and parallel to the superior surface of L3 (18.5 mm). The primary and secondary branches of the aorta and vena cava were also modeled to include the natural tethers that they provide to organs in the human body. The exterior skin of the model has been developed as a single surface from the external anthropometry laser scanning. This was modeled as a single part and was conditioned to remove artifact (arising mainly from breathing). This shell of the volunteer developed from the external scan data was also compared to medical image data by body region for validation. The surface area of the skin was 1.44 m^2, which is within 2% of estimates in the literature for a female of the same height and body weight (Burmaster 1998; Gehan and George 1970). The assembled model can be seen in Figure 4.

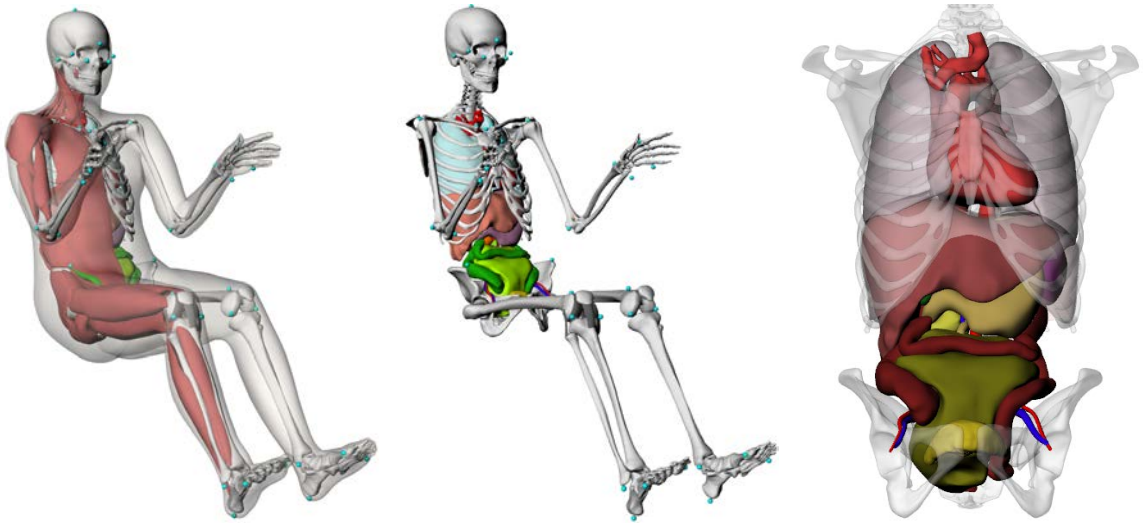

Figure 4. Assembled 3D F05 Occupant. Images show the full skeleton and all internal organs that will be explicitly represented. Bony landmark data is shown as blue points.

CONCLUSIONS

This study presents a comprehensive set of image and anthropometrical data of the F05. This included the use of state of the art imaging techniques, surface scanning, and 3D digitization for collection of bony landmark data. Ultimately, all bony structures and the majority of soft tissue data that will be modeled were obtained using medical images of this subject. In order to accurately assemble the structures, the full dataset was leveraged, where appropriate, to facilitate model development. Assembly of skeletal structures in the model coordinate system was completed using the external anthropometry dataset and bony structures placed in the seated CT scans. Seated uMRI scans were used for assembly of abdominal organs to ensure correct shape and position.

Height and weight requirements for the subject were taken from nominal values utilized for development of the Hybrid III F05 anthropomorphic test device (ATD). This approach was taken because the response of the subsequent finite element model of the F05 will ultimately be compared to the F05 ATD. This allows for direct comparison to an ATD that is already an integral part of the regulatory process for crash tests. However, subject recruitment was also heavily based on anthropomorphic measurements taken from a survey of U.S. armed service personnel, known as the U.S. Army Anthropometry SURvey (ANSUR) (Gordon et al. 1989). This dataset was ultimately used because of its large size and the comprehensive nature of the measurements it contains. While it is noted that the population reviewed as part of ANSUR is not necessarily equivalent to the average world anthropometry measurements, at the time of this study, it was the most complete and thorough dataset available. In total, the ANSUR study screened over 25,000 subjects and ultimately reported specific measurements on 2,208 women averaging 26.19 years old. While other data sources, such as the CAESAR anthropometry database were considered, there were a number of requirements for the current study that were not contained in the CAESAR database. By obtaining our own prospectively recruited data, we were able to obtain landmark and surface data in a controlled driving posture based on seating accommodation models. Additionally, medical image data from the same subject used for the anthropometry component was another requirement for this dataset that was not previously available.

Across the 15 anthropometric measurements recorded, the waist circumference had the largest deviation from the target. While a large deviation from the target anthropometry in this area can be problematic due to anticipated interaction with simulated countermeasures, like seatbelts or airbags, this is a body region that can be adjusted in the final model development. The deviation from the target waist circumference can be attributed to the amount of subcutaneous fat found in the volunteer. From a modeling perspective, disagreement in this measurement is manageable because subcutaneous fat tissue can be readily reduced in the CAD development stage without affecting the morphology of surrounding structures. In addition, for the final model, subcutaneous fat generally acts to serve as a passive transfer for energy in the dynamic loading simulations.

The assembled skeleton of the female model was also compared to a finite element model of the Hybrid III F05. The Hybrid III ATD model was obtained from Livermore Software Technology Corp (LSTC) and measurements were taken using nodal distances. For the observed anthropometry, the segmented F05 had an average deviation compared to the HIII F05 of 2.7%. The measurements used for the comparison can be seen in Figure 5.

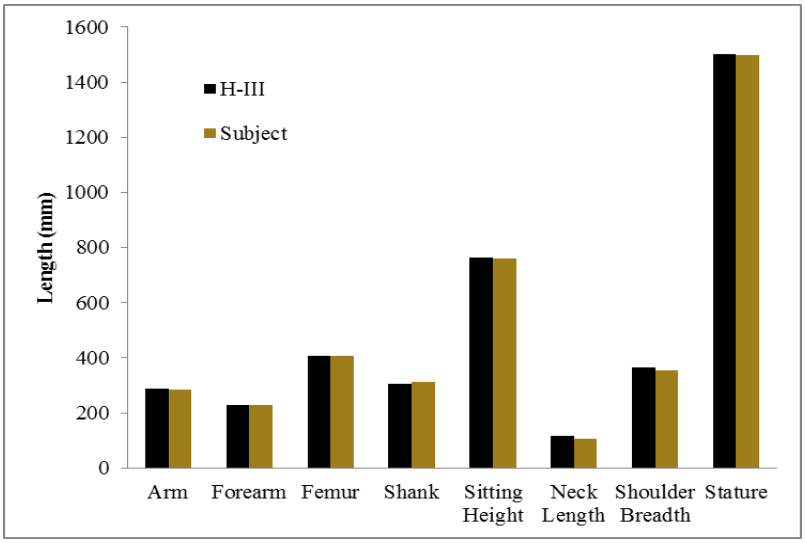

Figure 5. Comparison of F05 model assembly to F05 Hybrid III finite element model

While data for a specific anthropometric population such as the F05 is limited, comparisons were also made to literature sources where available. In 2004, Geraghty et al. published the normal distribution of female abdominal organ volumes from the 1st percentile to the 99th percentile using data obtained from clinical CT scans (Geraghty et al. 2004). However, this distribution is representative of organ volume specifically and not anthropomorphic percentiles. For example, a female that is anthropomorphically representative of the F05 does not necessarily have internal organs that fall at the 5th percentile of organ volumes. Despite this, it is currently the best data source to compare organ volumes of the F05. For modeling purposes, comparisons were made of organs relevant to crash induced injuries (CIIs). Typically, organs of interest for CIIs are considered the liver, spleen, left kidney and right kidney. The liver volume was found to closely match the 5th percentile and the right and left kidneys fell in the 10th percentile of organ volumes determined in the population based study. The spleen volume showed the largest deviation falling in the 20th percentile of female spleen volumes. However, it is difficult to assess whether or not these organ volumes are uncommon for a F05. For instance, it may not be unusual for anatomic variability to cause individuals of a select anthropometry to have widely ranging organ volumes.

Using supine CT data, measurements of cortical bone thickness were also obtained through segmentation. Due to limits imposed by the full width half max of the scanner, thickness measurements were limited to bones with diaphyseal measurements greater than 2.75 mm. This excluded bones, such as the ribs, with cortical thickness values throughout the structure that fall below the scanner cut-off that was used in this work. In these cases, cortical thickness values will be applied in the modeling phase using techniques from the literature (Kim et al. 2012; Li et al. 2010; Li et al. 2010). Ultimately, cortical thickness measurements were limited to specific long bones (humerus, radius, ulna, femur, fibula, tibia and femur) and compared to published data. The dataset was compared to a review of radiographic measurements of cortical bone published by Virtama et al (Virtama and Helela 1969). While the cortical thicknesses reported in this dataset are not specifically related to the F05, they do provide a good initial point of comparison. In each case, the literature values were obtained from 25 year old subjects and all values were taken from right limbs at specified, discrete locations. In general, the results compared favorably to Virtama and Helela.

One of the main limitations of this work was the sample size. However, the decision to take this approach was made pragmatically. The careful recruitment of one anthropometrically representative female allowed

resources to be allocated for the collection of an extensive amount of both medical image data and external surface data that would not have been feasible on a larger sample of subjects. By taking this approach, medical image data was available to validate results of the developed geometries.

This work has attempted to not only present the development of a small female finite element model, but also to provide geometric data that otherwise is limited in the literature. Data on the organ volumes and cortical thickness values of the small female can be used for future modeling applications. Also, detailed anthropometric landmarks will be useful for future reconstruction of small female models. This will also facilitate more accurate model to model comparisons. However, in order to more accurately evaluate the development of the F05, additional data pertinent to the small female is required. Future work will involve developing datasets specifically representative of the F05 population. For example, organ volumes specifically measured within the F05 population are necessary to draw a true comparison to a subject selected based on anthropometry. Similarly, cortical thickness measurements from anthropometrically representative females would be useful to increase the accuracy of fracture prediction within subsequently developed models.

The data and techniques outlined in this paper have focused on the assembly and validation of anatomical structures relevant to the modeling of CIIs, namely bony structures and organs. However, as seen in Figure 4, other structures designed to facilitate passive load transfer and promote accurate kinematics will also be modeled. Grouped CAD representations of muscle have been developed to reduce void space in the model. In addition, roughly 26 ligaments, tendons, and other cartilaginous tissues are targeted for inclusion in the final model (Gayzik et al. 2011). With regards to model development, cartilaginous tissue will be created during the meshing phase where possible, reducing the need for CAD representations. Because the dataset will ultimately be used for the evaluation of tissue response to blunt impact, much of the microstructure of the human body has not been included. This approach was taken since final model validation will be compared to empirical data obtained from experiments conducted at the organ or full-body levels.

This study presents a methodology and comprehensive dataset for the development of a 5^{th} percentile female finite element model. The data were collected using a multi-modality medical imaging protocol and a custom, adjustable buck for collection of external landmarks. The dataset is versatile and was obtained to accurately assemble the model in both the occupant and pedestrian postures. Preliminary segmentation work shows that volumetric organ data and cortical bone thickness from the prospectively recruited F05 subject reasonably matches available population based studies. Ultimately, these data will be used as part of a larger effort in developing a detailed finite element model of the 5^{th} percentile female for human injury prediction in vehicular crash.

ACKNOWLEDGEMENTS

Funding for this study was provided by the Global Human Body Models Consortium, LLC (GHBMC) through GHBMC Project Number: WFU-005. Support for CAD generation provided by Zygote Media Group, Inc. (American Fork, Utah).

REFERENCES

BEILLAS, P., LAFON, Y., SMITH, F. W. (2009) The effects of posture and subject-to-subject variations on the position, shape and volume of abdominal and thoracic organs. Stapp Car Crash J 53: 127-54.

BURMASTER, D. (1998) Lognormal distributions for skin area as a function of body weight. Risk Analysis 18 (1): 27.

DAVIS, M.L., ALLEN, B.C., GEER, C.P., STITZEL, J.D., AND GAYZIK, F.S. (2014) A Multi-Modality Image Set for the Development of a 5th Percentile Female Finite Element Model. Proc. International Research Council on Biomechanics of Injury.

DEWIT, J.A., AND CRONIN, D.S. (2012) Cervical Spine Segment Finite Element Model for Traumatic Injury Prediction. Journal of the Mechanical Behavior of Biomedical Materials 10: 138-150.

DUMA, S.M., SCHREIBER, P.H., MCMASTER, J.D., CRANDALL, J.R., BASS, C.R., AND PILKEY, W.D. (1999) Dynamic injury tolerances for long bones of the female upper extremity. Journal of anatomy 194 (3): 463-471.

EVANS, L. (2001) Female compared with male fatality risk from similar physical impacts. Journal of Trauma-Injury, Infection, and Critical Care 50 (2): 281-288.

GAYZIK, F.S., HAMILTON, C.A., TAN, J.C., MCNALLY, C., DUMA, S.M., KLINICH, K.D., AND STITZEL, J.D. (2009) A Multi-Modality Image Data Collection Protocol for Full Body Finite Element Analysis Model Development. SAE Technical Paper 2009-01-2261.

GAYZIK, F.S., MORENO, D.M., GEER, C.P., WUERTZER, S.D., MARTIN, R.S., AND STITZEL, J.D. (2011) Development of a Full Body CAD Dataset for Computational Modeling: A Multi-Modality Approach. Annals of Biomedical Engineering 39 (10): 2568-2583.

GAYZIK, F.S., MORENO, D.P., DANELSON, K.A., MCNALLY, C., KLINICH, K.D., AND STITZEL, J.D. (2012) External Landmark, Body Surface, and Volume Data of a Mid-Sized Male in Seated and Standing Postures. Annals of Biomedical Engineering 40 (9): 2019-32.

GEHAN, E.A., AND GEORGE, S.L. (1970) Estimation of human body surface area from height and weight. Cancer chemotherapy reports. Part 1 54 (4): 225-235.

GERAGHTY, E.M., BOONE, J.M., MCGAHAN, J.P., AND JAIN, K. (2004) Normal organ volume assessment from abdominal CT. Abdom Imaging 29 (4): 482-90.

GORDON, C.C., CHURCHILL, T., CLAUSER, C.E., BRADTMILLER, B., AND MCCONVILLE, J.T. (1989) Anthropometric survey of US army personnel: methods and summary statistics 1988. DTIC Document.

HAPPEE, R., RIDELLA, S., NAYEF, A., MORSINK, P., DE LANGE, R., BOURS, R., AND VAN HOOF, J. Mathematical human body models representing a mid size male and a small female for frontal, lateral and rearward impact loading. Proc. Proceedings of the 2000 International IRCOBI Conference on the Biomechanics of Impact, September 20-22, 2000, Montpellier, France.

HAYES, A.R., GAYZIK, F.S., MORENO, D.P., MARTIN, R.S., AND STITZEL, J.D. (2013) Abdominal Organ Location, Morphology, and Rib Coverage for the 5(th), 50(th), and 95(th) Percentile Males and Females in the Supine and Seated Posture using Multi-Modality Imaging. Ann Adv Automot Med 57: 111-22.

HAYES, A.R., VAVALLE, N.A., MORENO, D.P., STITZEL, J.D., AND GAYZIK, F.S. (2014) Validation of simulated chestband data in frontal and lateral loading using a human body finite element model. Traffic Inj Prev 15 (2): 181-6.

IWAMOTO, M., OMORI, K., KIMPARA, H., NAKAHIRA, Y., TAMURA, A., WATANABE, I., MIKI, K., HASEGAWA, J., OSHITA, F., AND NAGAKUTE, A. Recent advances in THUMS: development of individual internal organs, brain, small female and pedestrian model. Proc. Proceedings of 4th European LS Dyna Users conference, pp. 1-10.

KIM, Y.H., KIM, J.-E., AND EBERHARDT, A.W. (2012) A new cortical thickness mapping method with application to an in vivo finite element model. Computer methods in biomechanics and biomedical engineering (ahead-of-print): 1-5.

KIMPARA, H., IWAMOTO, M., AND MIKI, M. Development of a small female FEM model. Proc. Proc. JSAE spring congress, Issue, pp. 1-4.

KIMPARA, H., LEE, J.B., YANG, K.H., KING, A.I., IWAMOTO, M., WATANABE, I., MIKI, K. (2005) Development of a three-dimensional finite element chest model for the 5(th) percentile female. Stapp Car Crash J 49: 251-69.

KING, A.I., AND YANG, K.H. (1995) Research in biomechanics of occupant protection. Journal of Trauma-Injury, Infection, and Critical Care 38 (4): 570-576.

LI, Z., KINDIG, M.W., KERRIGAN, J.R., UNTAROIU, C.D., SUBIT, D., CRANDALL, J.R., AND KENT, R.W. (2010) Rib Fractures Under Anterior-Posterior Dynamic Loads: Experimental and Finite-Element Study. Journal of Biomechanics 43: 228.234.

LI, Z., KINDIG, M.W., KERRIGAN, J.R., UNTAROIU, C.D., SUBIT, D., CRANDALL, J.R., AND KENT, R.W. (2010) Rib fractures under anterior–posterior dynamic loads: experimental and finite-element study. Journal of biomechanics 43 (2): 228-234.

LI, Z., KINDIG, M.W., SUBIT, D., AND KENT, R.W. (2010) Influence of Mesh Density, Cortical Thickness and Material Properties on Human Rib Fracture Prediction. Medicine Engineering and Physics 32: 998-1008.

MACKAY, M., AND HASSAN, A.M. (1999) Age and gender effects on injury outcome for restrained occupants in frontal crashes: a comparison of UK and US data bases. Annual proceedings/Association for the Advancement of Automotive Medicine. Association for the Advancement of Automotive Medicine 44: 75-91.

MANARY, M., REED, M., FLANNAGAN, C., AND SHCHNEIDER, L. (1998) ATD Positioning Based on Driver Posture and Position. Stapp Car Crash J 42: 337.

MELVIN, J.W., HORSCH, J.D., MCCLEARY, J.D., WIDEMAN, L., JENSEN, J.L., AND WOLANIN, M. (1993) Assessment of air bag deployment loads with the small female hybrid III dummy. Safety 2010: 10-14.

MORRIS, C.R., ZUBY, D.S., AND LUND, A.K. (1998) Measuring airbag injury risk to out-of-position occupants. ESV16: 1036-1043.

SCHNEIDER, L., ROBBINS, D., PFLUG, M., AND SNYDER, R. (1983) Development of anthropometrically based design specifications for an advanced adult anthropometric dummy family, Vol 1., ed. N. US Department of Transportation.

SERRE, T., BRUNET, C., BRUYERE, K., VERRIEST, J.P., MITTON, D., BERTRAND, S., SKALLI, W. (2006) HUMOS (Human Model for Safety) Geometry: from one specimen to the 5th and 95th percentile. SAE Technical Paper 2006-01-2324.

SHIN, J., YUE, N., AND UNTAROIU, C.D. (2012) A finite element model of the foot and ankle for automotive impact applications. Ann Biomed Eng 40 (12): 2519-31.

SONI, A., AND BEILLAS, P. (2013) Modelling hollow organs for impact conditions: a simplified case study. Comput Methods Biomech Biomed Engin.

SUMMERS, L., HOLLOWELL, W.T., AND PRASAD, A. Analysis of occupant protection provided to 50th percentile male dummies sitting mid-track and 5th percentile female dummies sitting full-forward in crash tests of paired vehicles with redesigned air bag systems. Proc. Proceedings of the 17th International Technical Conference on the Enhanced Safety of Vehicles, Amsterdam, The Netherlands.

TOYOTA (2010) Documentation of Total Human Model for Safety (THUMS) AM50 Pedestrian/Occupant Model. Toyota Motor Corporation.

ULFARSSON, G.F., AND MANNERING, F.L. (2004) Differences in male and female injury severities in sport-utility vehicle, minivan, pickup and passenger car accidents. Accident Analysis & Prevention 36 (2): 135-147.

VEZIN, P., AND VERRIEST, J.P. Development of a set of numerical human models for safety. Proc. Proceedings of The 19th. International Technical Conference on the Enhanced Safety of Vehicles (ESV), Washington DC.

VIRTAMA, P., AND HELELA, T. (1969) Radiographic measurements of cortical bone: Variations in a normal population between 1 and 90 years of age. Acta Radiologica, Suplementum 293.

W.H.O (2013) Global status report on road safety. ed. W. H. Organization. World Health Organization, Geneva, Switzerland.

WELSH, R., AND LENARD, J. Male and female car drivers-difference in collision and injury risks. Proc. Proceedings of the Association for the Advancement of Automotive Medicine, 24-26 September, 2001.

YANG, K.H., HU, J., WHITE, N.A., KING, A.I., CHOU, C.C., AND PRASAD, P. (2006) Development of Numerical Models for Injury Biomechanics Research: A Review of 50 Years of Publications in the Stapp Car Crash Conference. Stapp Car Crash J 50: 429-90.